Available online at www.sciencedirect.com
SCIENCE DIRECT®
Journal of Organometallic Chemistry 690 (2005) 5353–5364
Journal of Organometallic Chemistry
www.elsevier.com/locate/jorganchem

Toward a general method for CCC *N*-heterocyclic carbene pincer synthesis: Metallation and transmetallation strategies for concurrent activation of three C–H bonds

Ramel J. Rubio, Gurusamy Thangavelu Senthil Andavan, Eike B. Bauer, T. Keith Hollis *, Joon Cho, Fook S. Tham, Bruno Donnadieu

Department of Chemistry, Physical Sciences 1, University of California, Riverside, CA 92521-0403, United States

Received 8 February 2005; received in revised form 27 April 2005; accepted 3 May 2005
Available online 27 June 2005

Abstract

A general solution to the preparation of pincer complexes that require the formation of two *N*-heterocyclic carbenes (NHC's) and the activation of an aryl C–H bond is reported. The reaction of a phenylene-bridged bis(imidazolium) salt with $Zr(NMe_2)_4$ generated the requisite CCC–NHC Zr pincer complex, which has been characterized by X-ray crystallography. Subsequent manipulation of the Zr coordination sphere by reaction with MeI demonstrated the robustness of the ligand geometry at Zr and led to the isolation and structural characterization of a CCC–NHC Zr triiodide pincer complex. A variation of the methodology has been applied to a saturated NHC analog to produce the corresponding CCC–NHC Zr pincer complex. Importantly, it has been found that CCC–NHC Zr pincer complexes can be generated in situ and transmetallated with an appropriate Rh source to generate CCC–NHC Rh pincer structures. These two methodologies, metallation of CCC–NHC precursors with transition metal amido complexes combined with transmetallation, hold great promise for opening general synthetic pathways to a wide variety of transition metal CCC–NHC pincer complexes.

Keywords: *N*-heterocyclic carbene; Pincer complex; Synthetic method; Zirconium complex; Rhodium complex

1. Introduction

Carbenes have a long history as intermediates in organic chemistry [1]. More recently, stable carbenes have been isolated and characterized [2], and *N*-heterocyclic carbenes (NHC's) have become ubiquitous in the field of catalysis [3]. They are found as ligands in a variety of catalysts for bond forming reactions such as hydrogenation [3,4], carbon–carbon [5], carbon–nitrogen [6] and olefin metathesis [7] with new reports appearing in almost every new journal issue [8]. Singlet carbenes are stronger σ-donors and dissociate less readily than phosphines thus generating more robust catalysts [7b]. This explosion of reports has led to interest in non-NHC carbenes and their use as ligands also [9].

Pincer complexes have been known since the early 1970's [10] and have been used recently as efficient catalysts for alkane dehydrogenation [11,12]. Pincer complexes are tridentate ligands that are bound to the metal via a central metal–carbon σ-bond and have donor atoms (D = O, S, N or P), which coordinate to the metal in a "pincer-like" manner **1**. One limitation of PCP pincer dehydrogenation catalysts was deactivation at elevated temperatures by C–P bond scission [13]. Since C–N bonds are typically stronger [14] we have been evaluating the possibility of using NHC's, as the

* Corresponding author. Tel.: +1 951 827 3024; fax: +1 951 827 4713.
E-mail address: keith.hollis@ucr.edu (T.K. Hollis).

0022-328X/$ - see front matter © 2005 Elsevier B.V. All rights reserved.
doi:10.1016/j.jorganchem.2005.05.007

donor atoms. A direct atom mapping of the pincer motif onto an NHC skeleton is illustrated in **2**.

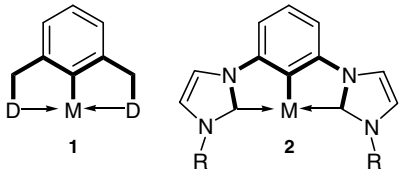

The synthesis of CCC–NHC pincer complexes is an area of increasing interest and need. Several groups have reported NHC pincer complexes related to **2**. Among these the most closely related in terms of molecular geometry are the pyridylene-bridged CNC–NHC pincer complexes **3** [15,16]. The synthesis of the pyridylene analogue **3** is straightforward since coordination of the pyridyl N requires no special conditions. Numerous complexes have been reported with Fe [16], Pd [17], Ru [15b], Rh [15c], Cr [15a,16], V and Ti [16]. The most closely related ligand system in terms of coordinating atoms is the xylylene-bridged CCC–NHC complexes **4** [18]. Since Pd is an excellent reagent for cyclometallation [19], the Pd derivative of **4** was the first and only one that has appeared in the literature. Attempts to prepare the Rh analogue were reported to yield no desired complex. In contrast to the pyridylene analogue **3**, the xylylene analogue **4** presents the same synthetic challenges as our ligand system **2**. Activation of the central aryl C–H bond along with the two NHC C–H bonds has proven to be a daunting task. Two deprotonations and a C–H activation concurrently are required and thus have limited the examples of such complexes. Examples of a pyridylene-bridged ligand that also incorporates the methylene spacers **5** have been reported also [18a,20].

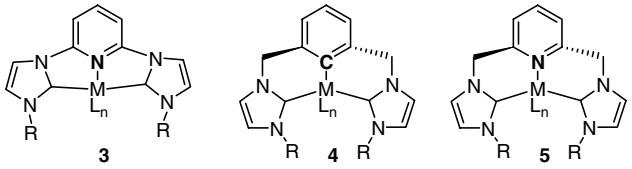

Recently, we reported the efficient one pot synthesis of 1,3-bis(imidazole) benzene (**6**, Scheme 1) employing a Cu-catalyzed aryl amination reaction followed by alkylation yielding bis(imidazolium) salts that are the precursors for the generation of **2** [21]. We report here the one step metallation of these bis(imidazolium) salts in the synthesis of CCC–NHC Zr pincer complexes of the type **2**. Subsequent transmetallation of a CCC–NHC Zr pincer complex to Rh generating the late transition metal CCC–NHC Rh pincer complex is also reported. The combination of these methodologies promises access to CCC–NHC pincer complexes across the transition series.

2. Synthetic design

A successful synthesis of CCC–NHC pincer complexes such as **2** and **4** requires two different and often mutually incompatible reagents. To accomplish the synthesis two equivalents of base are needed for the generation of the NHC's, and typically an electrophile is needed for the activation of the aryl C–H bond. Usually, an electrophile and a base are mutually exclusive due to Lewis acid/Lewis base quenching. This incompatibility has been the source of difficulty in the development of a direct, general preparation of CCC–NHC pincer complexes. A reagent that could function as an electrophile and a base simultaneously became our goal. $Zr(NMe_2)_4$ was thought to fulfill these requirements since it has an electron deficient Zr center. Based on a recent reports by Fryzuk and Cowley groups [22–24] it was evident that Group 4 amido complexes were sufficiently basic to activate the imidazolium precursor. We reasoned that the Zr–NHC formed in our ligand system would place the electrophilic Zr center in a position that would activate the aryl C–H bond. The basic amido ligand would function as a built-in base for deprotonation. Metal amido complexes have been reported recently to deprotonate organic compounds for the synthesis of organometallic complexes [25]. Further, we rationalized that the known facile transmetallation of Zr to late transition metals would allow us to access other complexes of the new ligand architecture [26].

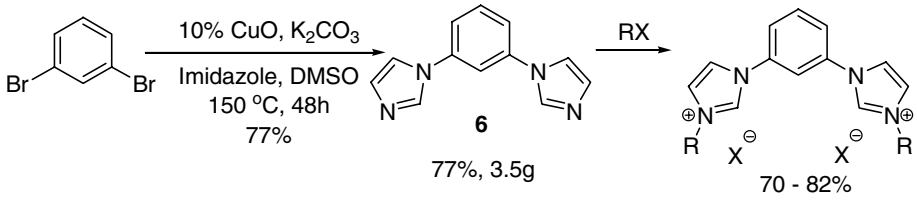

Scheme 1. Efficient synthesis of 1,3-phenylene ligand precursors.

3. Results and discussion

3.1. Metallation of ligand precursors with $Zr(NMe_2)_4$

3.1.1. Preparation, characterization and molecular structure of 2-(1,3-bis(N-butylimidazol-2-ylidene)-phenylene)bis(dimethylamido)(iodo) zirconium (IV) (**8**) and 2-(1,3-bis(N-butylimidazol-2-ylidene)-phenylene)(dimethylamido)bis(iodo) zirconium (IV) (**9**)

The recent report employing $Zr(NMe_2)_4$ to prepare a Zr–NHC complex inspired us to consider this reagent [22]. Combining salt **7** (R = *n*-Bu, X = I) with $Zr(NMe_2)_4$ and CH_2Cl_2 at room temperature produced CCC–NHC Zr pincer **8** as illustrated in Scheme 2 [27]. The addition of one equivalent of $Zr(NMe_2)_4$ to **7** resulted in the formation of a complex spectrum that still contained an imidazolium C–*H* signal at 11.22 ppm in the ^{1}H NMR spectrum. Addition of excess $Zr(NMe_2)_4$ resulted in the formation of a single product. Our optimized conditions involve the reaction of 2.5 equivalents of $Zr(NMe_2)_4$ with bis(imidazolium) salt **7** (R = *n*-Bu, X = I) to produce clean, quantitative conversion to a single product as depicted in Scheme 2. However, clean loss of the imidazolium protons and of one aryl proton was observed by ^{1}H NMR spectroscopy indicating the formation of the pincer complex. The ^{13}C NMR spectrum shows clear evidence for the formation of a single product with a Zr–NHC signal at 188.9 ppm [28]. Particularly noteworthy was the signal for the methylene bonded to the N of the NHC. In the crystal structure described below (see Fig. 1) the hydrogens of the methylene are diastereotopic and should produce to two signals in the ^{1}H NMR spectrum. Diastereotopic signals are not observed at room temperature for **8** or any other Zr complex described herein although broadening was observed at −80 °C [29]. The data were consistent with rapid exchange at the Zr center in **8** due to the presence of excess Zr amido. Attempted sublimation to remove excess amido reagent failed due to the presence of $Zr(NMe_2)_{4-x}I_x$, which are not sufficiently volatile under the conditions we were able to achieve. Separation of the bulk product from excess Zr amido proved difficult to achieve. Therefore, the crude product was reacted further to obtain a triiodo complex that was isolated (vide infra, Scheme 3).

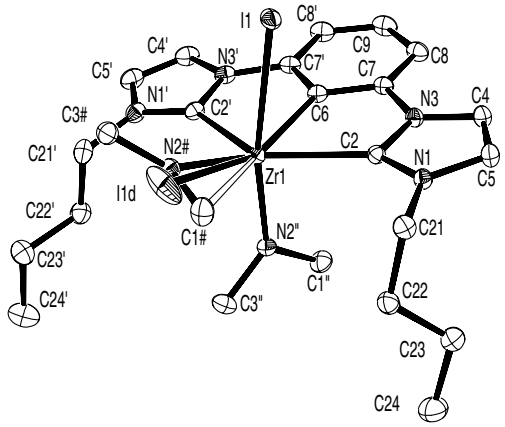

Fig. 1. ORTEP diagram (50% probability ellipsoids, hydrogens omitted for clarity) of complex **8** and **9**. A solid solution was observed in the crystal with 91% of the crystal showing two amido groups and one iodide group and 9% of the crystal showing one amido group and two iodides.

Despite the lack of separation procedures an X-ray quality crystal of **8** was grown from the reaction mixture. The crystal was a solid solution with 9% of the sites containing the diiodo mono-amido complex **9** the expected initial product, which was converted to **8** by exchange between the various amido species present [30]. An ORTEP view of the molecular structure is illustrated in Fig. 1, and crystallographic data are listed in Table 2. The overall molecular geometry is a distorted octahedron. The meridonal pincer ligand requires bond angles at Zr that are reduced relative to the idealized values and produces four fused five-membered rings that are

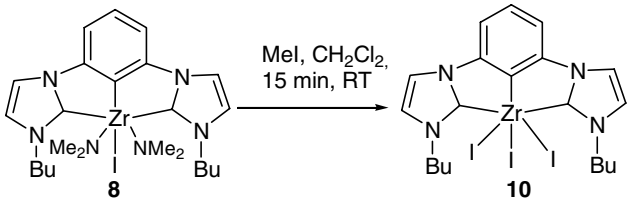

Scheme 3. Preparation and isolation of a CCC–NHC Zr pincer reagent for synthesis.

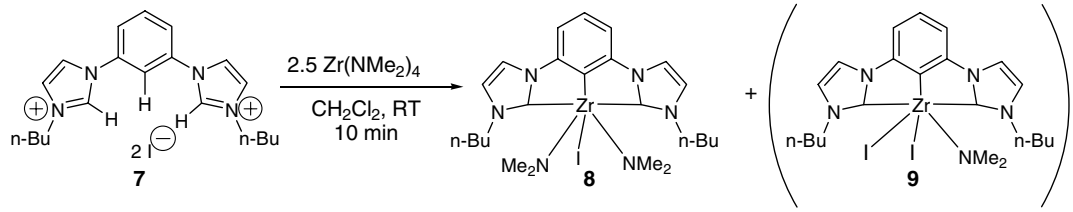

Scheme 2. Synthesis of CCC–NHC Zr pincer complex of **8**. Complex **9** was identified in the X-ray crystal structure and occupies 9% of the crystal sites.

coplanar. A summary of the bond distances and angles appears in Table 1. The Zr–C^{aryl} bond length is 2.3244(10) Å, which is normal for Zr–C^{aryl} bonds [31]. The Zr–C^{NHC} bond distances, 2.4256(10) and 2.3990(11) Å are longer than the value recently reported by Fryzuk (2.391(5) Å) [22] and are shorter than the *trans*-NHC–Zr bonds reported by Erker (2.432(3) Å) [24]. The axial Zr–I bond distance in **8** was 3.07615(18) Å demonstrating a stronger *trans* influence for the π-donating amido group compared to the aryl group, since the equatorial Zr–I distance in **9** was 2.7397(11) Å [32]. The Zr–N bond distances are 2.0524(10) for the axial position and 2.0793(10) Å for the equatorial position. The equatorial N (N2#) in **8** was skewed from the expected position based on the C^{aryl}–Zr–N angle of 151° and the Zr–N–C(1#) angle of 98°. It was pyramidalized to a greater extent than the axial amido ligand. This distortion appears to be caused by two reinforcing factors. The methylene carbon (C21′) of the butyl group and the methyl carbon (C3#) of the amido group are 3.5 Å apart, the van der Waals minimum for Me–Me attractive interactions [33]. The other factor appears to be a C–H agostic interaction with the Zr center that results in the angle distortions. The Zr···C distance of 2.690 Å and the Zr···H distance of 2.433 Å are indicative of an agostic interaction. These distances and angles are smaller than those found in recently reported (pyrrolyl)Zr amido complexes (Zr···C = 2.84 Å, Zr···H = 2.61 Å) for which an agostic interaction was claimed [34].

Table 1
Selected bond lengths (Å) and bond angles (°) for CCC–NHC Zr pincer complex (**8**); CCC–NHC Zr pincer complex (**9**); CCC–NHC Zr pincer triiodide (**10**); CCC–NHC Rh pincer complex (**14**)

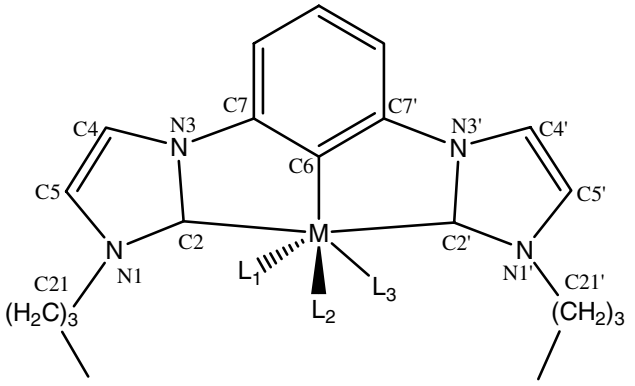

	8	9	10	14
Distances				
M–C2	2.4256(10)	2.4256(10)	2.334(3)	2.063(4)
M–C2′	2.3990(11)	2.3990(11)	2.335(3)	2.061(4)
M–C6	2.3244(10)	2.3244(10)	2.298(3)	1.943(4)
M–I (ax)	3.07615(18)	3.07615(18)	2.8087(5)	2.6694(5)
			2.8160(5)	2.6567(5)
M–I (eq)		2.7397(11)	2.8659(5)	2.8366(5)
M–*N* (amido) (ax)	2.0524(10)	2.0524(10)		
M–*N* (amido) (eq)	2.0793(10)			
N1–C21	1.4645(14)	1.4645(14)	1.460(5)	1.478(5)
N1′–C21′	1.4618(17)	1.4618(17)	1.448(5)	1.490(5)
N1–C2	1.3499(14)	1.3499(14)	1.356(4)	1.352(5)
N1′–C2′	1.3525(15)	1.3525(15)	1.343(4)	1.354(5)
N3–C2	1.3638(14)	1.3638(14)	1.362(4)	1.371(5)
N3′–C2′	1.3687(15)	1.3687(15)	1.362(4)	1.384(5)
C5–C4	1.3561(17)	1.3561(17)	1.350(6)	1.322(6)
C5′–C4′	1.351(2)	1.351(2)	1.331(6)	1.336(6)
C5–N1	1.3861(14)	1.3861(14)	1.374(5)	1.373(5)
C5′–N1′	1.3846(16)	1.3846(16)	1.385(5)	1.364(5)
C4–N3	1.3841(15)	1.3841(15)	1.373(5)	1.367(5)
C4′–N3′	1.3799(15)	1.3799(15)	1.386(4)	1.374(5)
Angles				
C2–M–C2′	136.04(4)	136.04(4)	136.74(12)	156.98(16)
C6–M–C2	68.27(4)	68.27(4)	68.49(12)	78.56(18)
C6–M–C2′	67.78(4)	67.78(4)	68.49(12)	78.54(17)
C7–N3–C2	119.62(9)	119.62(9)	117.7(3)	117.1(4)
C7′–N3′–C2′	118.70(9)	118.70(9)	118.2(3)	117.1(4)
N1–C2–N3	103.95(9)	103.95(9)	103.9(3)	103.8(4)
N1′–C2′–N3′	103.60(9)	103.60(9)	104.6(3)	103.8(4)
C2–N1–C5	111.74(9)	111.74(9)	110.8(3)	110.8(4)
C2′–N1′–C5′	111.55(11)	111.55(11)	110.5(3)	112.1(4)
C2–N3–C4	111.53(9)	111.53(9)	111.8(3)	110.5(4)
C2′–N3′–C4′	111.73(10)	111.73(10)	110.8(3)	111.7(4)

Refer to above diagram for a generalized numbering scheme. L_1, L_2, L_3 = I or NMe_2.

3.1.2. Preparation, characterization and molecular structure of 2-(1,3-bis(N-butylimidazol-2-ylidene)-phenylene)tris(iodo) zirconium (IV) (*10*)

Because of the difficulty encountered trying to isolate the Zr pincer complex from excess $Zr(NMe_2)_4$, further derivatization was accomplished while also decomposing the excess amido reagent. Excess methyl iodide was added to **8** at room temperature to give compound **10** in 87% isolated yield (Scheme 3). The ^{13}C NMR spectrum showed a diagnostic metallated carbene peak at 195.5 ppm. A crystal of **10** was obtained from a saturated solution of benzene. The single crystal X-ray diffraction study confirmed the formation of a tridentate CCC pincer complex, and the ORTEP plot is presented in Fig. 2 and crystallographic data are listed in Table 2.

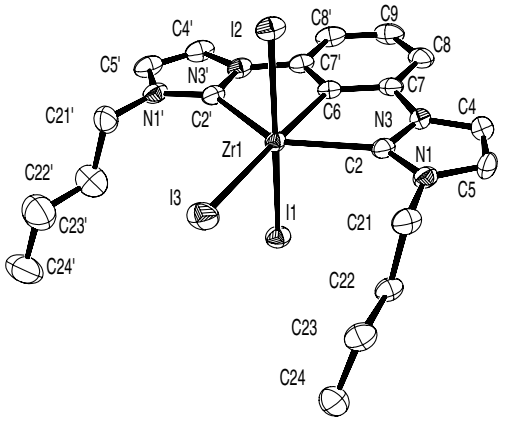

Fig. 2. ORTEP diagram of **10** (50% probability, hydrogen atoms and solvent of crystallization, C_6H_6, omitted for clarity).

Table 2
Summary of crystallographic data for compounds **8**, **9**, **10**, **14**

	8, **9**	**10**	**14**
Empirical formula	$[C_{20}H_{25}N_4ZrI[N(CH_3)_2]_2]$ (91%) $[C_{20}H_{25}N_4ZrI_2N(CH_3)_2]$ (9%) (C23.83 H36.49 I1.09 N5.91 Zr)	$C_{26}H_{31}I_3N_4Zr$	$C_{20}H_{25}I_2N_4Rh$
Formula weight	627.72 (91%) 710.55 (9%) (634.76)	871.47	678.15
T (K)	100(2)	100(2)	100(2)
Wavelength (Å)	0.71073	0.71073	0.71073
Crystal system	Monoclinic	Monoclinic	Monoclinic
Space group	$P2(1)/c$	$P2(1)/n$	$P2(1)/c$
Unit cell dimensions			
a (Å)	10.3724(5)	14.863(2)	12.4710(10)
b (Å)	11.8315(5)	9.0355(14)	14.8333(12)
c (Å)	21.6021(10)	22.857(4)	13.1292(11)
α (°)	90	90	90
β (°)	98.058(2)	104.273(2)	117.3690(17)
γ (°)	90	90	90
V (Å^3)	2624.9(2)	2974.7(8)	2156.9(3)
Z	4	4	4
D_c (Mg/m^3)	1.606	1.946	2.088
Absorption coefficient (mm^{-1})	1.717	3.504	3.667
$F(000)$	1274	1656	1296
Crystal size (mm)	$0.41 \times 0.33 \times 0.10$	$0.22 \times 0.09 \times 0.06$	$0.20 \times 0.16 \times 0.06$
Theta range for data collection (°)	1.90 to 36.32	1.48 to 26.37	1.84 to 30.50
Index ranges	$-17 \leqslant h \leqslant 16$, $-19 \leqslant k \leqslant 19$, $-35 \leqslant l \leqslant 35$	$-18 \leqslant h \leqslant 18$, $-11 \leqslant k \leqslant 11$, $-28 \leqslant l \leqslant 28$	$-17 \leqslant h \leqslant 15$, $0 \leqslant k \leqslant 21$, $0 \leqslant l \leqslant 18$
Reflections collected	103 964	21 289	7627
Independent reflections (R_{int})	12 730 (0.0254)	6083 (0.0264)	6564 (TWIN N/A)
Completeness to θ	100.0% (36.32°)	99.9% (26.37°)	99.8% (30.50°)
Absorption correction	Semi-empirical from equivalents	Semi-empirical from equivalents	Semi-empirical from equivalents
Maximum and minimum transmission	0.8443, 0.5373	0.8069, 0.5196	0.8210, 0.5334
Refinement method	Full-matrix least-squares on F^2	Full-matrix least-squares on F^2	Full-matrix least-squares on F^2
Data/restraints/parameters	12 730/0/350	6083/16/333	6564/0/245
Goodness-of-fit on F^2	1.072	1.025	1.021
Rotational twin	N/A	N/A	180° rotation about real axis 101
Final R indices [$I > 2\sigma(I)$]			
R_1	0.0223	0.0252	0.0322
wR_2	0.0550	0.0542	0.0608
R indices (all data)			
R_1	0.0271	0.0366	0.0609
wR_2	0.0572	0.0577	0.0626
Largest difference peak and hole (e Å^{-3})	2.789, −1.287	1.320, −0.843	1.782, −1.284

In the solid state the zirconium adopts a distorted octahedral geometry. The metal carbene distances are 2.334(3) and 2.335(3) Å, for C(2) and C(2′), respectively. These bond distances are similar to those reported in the literature. The Zr–C^{aryl} bond distance is 2.298(3) Å, which is consistent with other Zr–phenyl complexes [35]. The two iodides in the axial positions have Zr–I bond lengths of 2.8087(5) and 2.8160(5) Å. The equatorial Zr–I(3) bond length of 2.8659(5) Å demonstrates the greater *trans* influence of the aryl versus and iodo group. Additional geometric data are listed in Table 1. The potential of **10** as a starting material for further elaboration and catalyst development is tremendous. Exploring **10** as a non-metallocene complex for olefin polymerization is of special interest [36].

*3.1.3. Synthesis of 2-(1,3-di(N-ethyl-4,5-dihydroimidazol-2-ylidene)phenylene) tris(dimethylamido)-zirconium (IV) (**12**)*

Saturated NHC's are considerably more basic than the corresponding unsaturated NHC's [37]. Therefore, we sought to establish that the metallation methodology would work in these systems (Scheme 4). The successful metallation of the saturated systems will allow access to chiral complexes, a necessary prerequisite for the development of asymmetric catalysts.

The desired bis(imidazolinium) salt was prepared employing standard procedures from 1,3-diaminobenzene. The diamine was reacted with *N*-acetyl-glycine under standard amide formation conditions producing the tetraamide [38] that was reduced [39] and cyclized following the literature procedures as illustrated in Scheme 4 [40]. Upon exchange of counter ions with $Na(BPh_4)$ solid salt **11** was obtained. Attempted metallation of salt **11** under the standard conditions of 2.5 equivalents of $Zr(NMe_2)_4$ in CD_2Cl_2 did not produce clean spectra. When the amount of zirconium reagent was increased to 5 equivalents, clean ^1H and ^{13}C NMR spectra were obtained indicating the formation of a single product. The requirement of additional $Zr(NMe_2)_4$ is attributed to the lack of supporting ligands (i.e. BPh_4^- is the counter ion for salt **11** compared to halogens in other cases). Although a clean product was formed additional spectral analyses revealed the desired product was not obtained [41]. Next benzene was evaluated as a solvent for the reaction. Combining salt **11** and five equivalents of $Zr(NMe_2)_4$ and refluxing in benzene for 40 min produced an insoluble oil. Increasing the reaction time to 90 min produced an identical outcome. Removal of the supernatant followed by addition of CD_2Cl_2 allowed the collection of NMR data consistent with the desired product except that each peak was duplicated, a problem observed in other systems. Reaction time did not change the ratio of the two products. The NMR spectral data are consistent with CCC pincer carbenes **8** and **10**, which have been unambiguously established by X-ray crystallography. DEPT-135 experiments confirm the loss of the aryl C–H proton and formation of the CCC–NHC Zr pincer carbene. Reasoning that the dimethyl amine produced in the reaction might be responsible for generating alternate coordination spheres at Zr, it was decided to add a base that would deprotonate the amine. Consequently, mesityl lithium [42] was added to salt **11** for 10 min prior to the addition of $Zr(NMe_2)_4$. The mixture was refluxed for 30 min yielding an oil. The supernatant was decanted. Addition of CD_2Cl_2 and collection of the ^1H and ^{13}C NMR spectra revealed only one set of peaks corresponding to the minor product observed in the first reaction. This product was formulated as the tris(amido) complex **12**. Extension to readily available chiral amino acids will allow access to an unprecedented array of chiral CCC–saturated-NHC pincer complexes.

3.2. Transmetallation to rhodium

*3.2.1. Synthesis of 2-((1,3-bis(N-butylimidazol-2-ylidene)phenylene)-(dimethylamido)bis(iodo) rhodium(III) (**13**) and bis(2-(1,3-bis(N-butylimidazol-2-ylidene)phenylene))bis(μ²-iodo) dirhodium(III) (**14**)*

Many reaction conditions were evaluated to prepare late transition metal pincer complexes directly with little tractable material being obtained. Ag carbene complexes have been demonstrated to transmetallate effectively [43]. There is ample precedent for the transmetallation of Zr–C bonds to late transition metals especially when Pd is involved [44]. But, Pd readily undergoes cyclometallation and is, therefore, of less interest. The precedent for transmetallation to Rh is less well established [45]. Transmetallation to Rh was desired because the formation of the

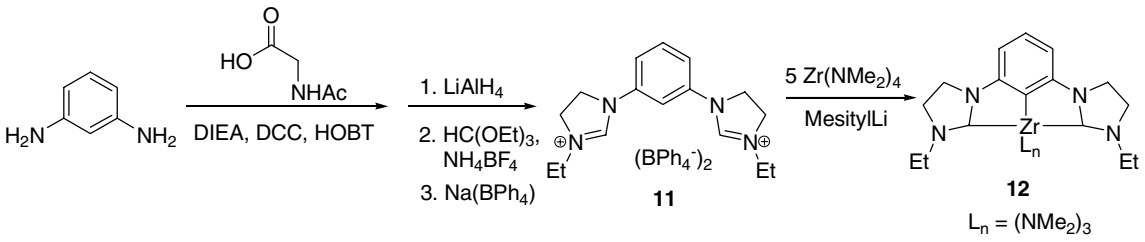

Scheme 4. Synthesis of 1,3-phenylene bis(imidazolinium) salts **11**, and metallation with $Zr(NMe_2)_4$ producing the CCC–saturated-NHC pincer complex **12**.

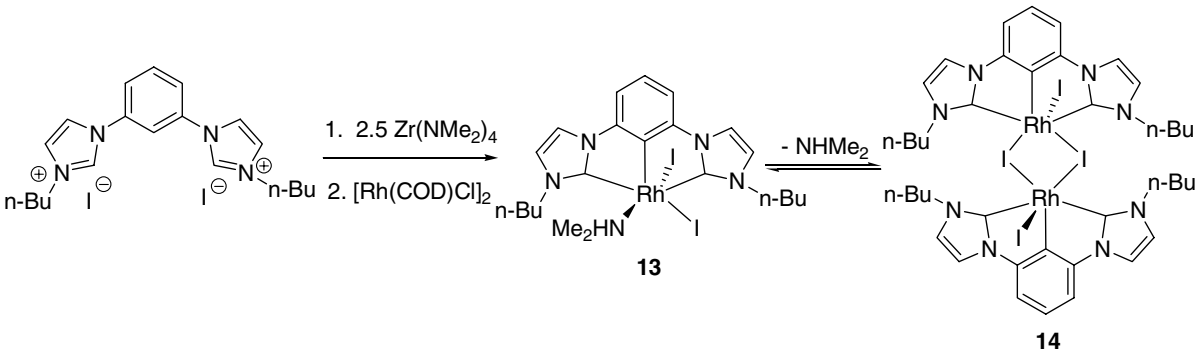

Scheme 5. Transmetallation from Zr to Rh in the preparation of late transition metal CCC–NHC pincer complexes.

product would be clearly observable by the Rh–C coupling in the ^{13}C NMR spectrum and because of our inherent interest in the Group 9 complexes. The Zr pincer complex **8** was prepared in situ in CH_2Cl_2 and combined with $[Rh(COD)Cl]_2$ in a 1:1 ratio of Rh:ligand as illustrated in Scheme 5. A new set of signals appeared in the ^{13}C NMR spectrum with a Rh–NHC doublet at 173.7 ppm ($J = 39$ Hz) and the Rh–C^{aryl} doublet at 150.8 ppm ($J = 40$ Hz). Despite repeated attempts only ~50% conversion to the Rh complex was observed with the remainder of the Zr complex intact. Attempting the reaction in THF resulted in an identical outcome. The solvent was removed, and a ^1H NMR collected in $CDCl_3$ from which an X-ray quality crystal grew by slow evaporation indicating a Rh(III) complex had been formed (**14**, Fig. 3). The oxidant and timing of the oxidation was unknown. The reaction was repeated and a sample was reacted with I_2 with the intent of facilitating the oxidation to provide direct access to the Rh(III) complex. ^{13}C NMR spectroscopy revealed an identical spectrum for the sample treated with I_2 to that obtained as a mixture during transmetallation. But, the process of reaction with I_2 and work-up had removed the excess Zr species. ^1H NMR spectroscopy now revealed a doublet of doublets for coordinated $HNMe_2$ at 1.78 ppm ($J = 1.5$, 4.5 Hz) for the CCC–NHC Rh pincer complex **13**. Additionally the methylene groups attached to the heterocycle are diastereotopic indicating that the octahedral geometry of the system as illustrated for **13**. Mass spectral analysis (LSIMS) of the product revealed peaks at $m/z = 724$ for $[M]^+$, $m/z = 596$ for the fragment $[M - I]^+$, $m/z = 679$ for $[M - NHMe_2]^+$ and $m/z = 551$ for $[M - I - (NHMe_2)]^+$ clearly establishing the molecular structure. The ammine complex **13** and the iodo-bridged dimer **14** were in equilibrium, and $NHMe_2$ was lost during the slow evaporation producing the crystals of **14**.

It was surmised that half of the Rh was involved in the oxidation to the Rh(III) complex. Therefore, an experiment was performed employing a Rh:ligand ratio of 2:1. The result was complete transmetallation to Rh and quantitative formation of **13** as determined by ^1H and ^{13}C NMR spectroscopy. The exact nature of the

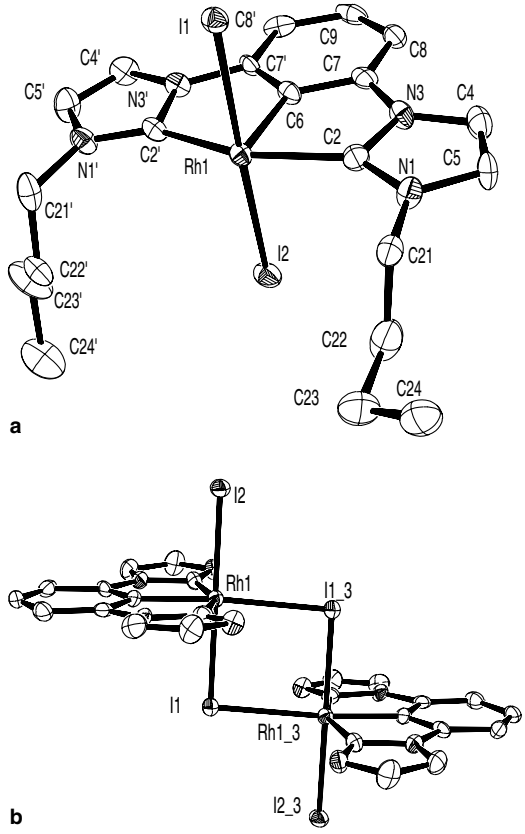

Fig. 3. (a) ORTEP plot (50% probability, hydrogens omitted for clarity) of the asymmetric unit of CCC–NHC Rh pincer complex **14**. (b) ORTEP plot (50% probability, hydrogens and carbons of the butyl groups omitted for clarity) of the edge-on view of the iodo-bridged Rh dimer structure that completes the octahedron of each molecule. Rh–Rh = 4.01 Å.

reduction product has yet to be determined. Clearly the strong meridonal σ-donating CCC–NHC pincer ligand favors the higher oxidation state Rh(III). Transmetallation to Rh(III) sources is under investigation, but has yet to be as successful as Rh(I).

An ORTEP plot of the molecular structure of **14** is depicted in Fig. 3 and crystallographic data are listed in Table 2. Both the asymmetric unit and the μ-iodo structure are illustrated. The dimer was generated by

an inversion center in the crystal. The Rh–Rh distance of 4.01 Å is well beyond bonding distance and is similar to other iodo bridged dimers [46]. Details of the geometry are included in Table 1.

4. Conclusions

In conclusion, a new CCC–NHC pincer ligand architecture has been established for Zr and Rh complexes. A new and general metallation methodology based on metal amido complexes that serve as bases and are electrophile has been demonstrated for CCC–NHC ligand and transition metal complex preparation. Further, transmetallation of the early transition metal CCC–NHC complexes to late transition metals has been established. These combined methodologies represent a new and general solution to the CCC–NHC complex synthesis and metallation problem, which has broad implications. Catalytic trials of with the CCC–NHC Rh pincer complexes are underway.

Many transition metal amido complexes are available thus making the metallation strategy demonstrated here widely applicable [47]. Preliminary results with Ti or Ta amido complexes indicate metallation as reported for Zr and will be reported in due course [48]. Preparation of chiral variants of the CCC–saturated-NHC complexes is underway. Improvements in the isolation of the primary metallation products are being sought.

5. Experimental

5.1. General considerations and materials

Unless otherwise noted, all manipulations were carried out under an inert atmosphere of Ar with the use of standard Schlenk, vacuum line, and glove box techniques. Dry oxygen-free solvents were used [49]. All deuterated solvents were filtered through basic alumina before dissolving the samples. NMR spectra were recorded on a Bruker Avance 300(300.132 MHz), Varian Inova (500.140 MHz and 300.053 MHz) instruments; Chemical shifts reported are relative to tetramethylsilane (0^{TM}), and were referenced by assigning the residual solvent peak. $[Rh(COD)Cl]_2$ and $Zr(NMe_2)_4$ were purchased from Strem® Chemicals and were used as received.

5.2. Synthesis and characterization of imidazolium and imidazolinium salts: ligand precursors

5.2.1. Synthesis of 1,3- bis(1-butylimidazolium)benzene diiodide (7)

1,3-Bis(imidazole)benzene (0.840 g, 4.00 mmol), 1-iodobutane (2.94 g, 16.0 mmol), and toluene (8 mL) were reacted in a sealed tube at 150 °C for 8 h. The suspension was then allowed to reach room temperature, and the contents were washed with THF (3 × 10 mL). The residue was dried under high vacuum to obtain **7** as a yellow solid (1.78 g, 77%): ^{1}H NMR (CD_2Cl_2): δ 11.27 (s, 2H), 8.96 (t, J = 2.1 Hz, 1H), 8.46 (t, J = 2.1 Hz, 2H), 8.14 (dd, J = 8.1 and 2.1 Hz, 2H), 7.89 (t, J = 8.4 Hz, 1H), 7.5 (t, J = 2.1 Hz, 2H), 4.46 (t, J = 7.5 Hz, 4H), 2.05 (pseudo-quintet, J = 7.5 Hz, 4H), 1.47 (pseudo-sextet, J = 7.5 Hz, 4H), 1.02 (t, J = 7.5 Hz, 6H); ^{13}C{^{1}H} NMR (75 MHz, DMSO-d_6): δ 137.6, 133.7, 127.2, 125.4, 124.5, 122.9, 117.6, 51.2, 32.9, 20.7, 15.2.

5.2.2. Synthesis of imidazolinium bis(tetraphenylborate) (11)

5.2.2.1. Preparation of 2-acetylamino-N-[3-(2-acetylamino-acetylamino)-phenyl]-acetamide. 1,3-Diaminobenzene (5.00 g, 46.2 mmol), *N*-acetylglycine (11.4 g, 97.1 mmol), 1-hydroxybenzotriazole (13.12 g, 97.1 mmol), *N*, *N*-diisopropylethylamine (16.9 mL, 97.1 mmol) and DMF (250 mL) were combined. *N*, *N*-dicyclohexylcarbodiimide (20.0 g, 97.1 mmol) was added at 0 °C. The reaction was stirred at 0 °C for 2 h and at room temperature overnight. A white precipitate was separated by filtration. The filtrate was concentrated to minimum volume, and CH_2Cl_2 (400 mL) was added yielding a white precipitate (13.0 g, 92%): ^{1}H NMR (DMSO-d_6): δ 9.97 (s, 2H), 8.20 (t, J = 5.7 Hz, 2H), 7.87 (s, 1H), 7.18–7.29 (m, 3H), 3.85 (d, J = 5.7 Hz, 4H), 1.88 (s, 6H); ^{13}C{^{1}H} (75 MHz, DMSO-d_6): δ 169.9, 168.0, 139.2, 129.0, 114.3, 110.3, 42.8, 22.5: MS(LSIMS) m/z 307.1411 $M + H^+$ 307.1406 calcd for $[C_{14}H_{19}N_4O_4]$.

5.2.2.2. Preparation of N,N′-bis-(2-ethylamino-ethyl)-benzene-1,3-diamine. 2-Acetylamino-*N*-[3-(2-acetylamino-acetylamino)-phenyl]-acetamide (520 mg, 1.69 mmol) and THF (40 mL) were combined and cooled to 0 °C, lithium aluminum hydride (642 mg, 16.90 mmol) was then added slowly. The mixture was stirred at room temperature for 1 h and refluxed overnight. After cooling to room temperature a saturated Na_2SO_4 solution (50 mL) was added. The solution was extracted with CH_2Cl_2 (3 × 50 mL) and combined organic layers were dried over $MgSO_4$. The dried organic layer was concentrated to give *N*,*N*′-bis-(2-ethylamino-ethyl)-benzene-1,3-diamine (366 mg, 87%) as a brown oil. ^{1}H NMR ($CDCl_3$): δ 6.96 (t, J 8.1 Hz, 2H), 6.02 (d, J = 8.1 Hz, 1H), 5.93 (s, 1H), 3.19 (t, J = 5.7 Hz, 4H), 2.85 (t, J = 5.7 Hz, 4H), 2.66 (q, J = 6.9 Hz, 4H), 1.10 (t, J = 6.9 Hz, 6H); ^{13}C{^{1}H} (75 MHz, $CDCl_3$): δ 149.4, 129.6, 102.5, 97.1, 48.4, 43.6, 43.3, 15.1: MS(LSIMS) m/z 251.2234, $[M + H]^+$ 251.2236 calcd for $[C_{14}H_{26}N_4]$.

*5.2.2.3. Preparation of 1,3-bis(1-ethylimidazolium)benzene bis(tetraphenylborate) (**11**).* *N*,*N*′-Bis-(2-ethylamino-ethyl)-benzene-1,3-diamine (350 mg, 1.40 mmol), triethyl orthoformate (0.465 mL, 2.80 mmol) and ammonium tetrafluoroborate (302 mg, 2.80 mmol) was combined. The mixture was stirred at 120 °C for 3 h. The reaction was concentrated, and a brown sticky oil was obtained. Methanol (20 mL) and sodium tetraphenylborate (479 mg, 1.40 mmol) was added and the reaction was stirred at room temperature for 3 h. An orange precipitate was collected. Recrystallization from acetone/isopropanol yielded pure product (535 mg, 42%): ^{1}H NMR (DMSO-d_6): δ 9.34 (s, 2H), 7.59 (t, J = 8.1 Hz, 2H), 7.30 (dd, J = 1.8 and 8.1 Hz, 1H), 7.24 (t, J = 1.8 Hz, 1H), 7.18 (m, 16H), 6.92 (t, J = 7.2 Hz, 16H), 6.79 (t, J = 7.2 Hz, 8H), 4.34 (t, J = 10.2 Hz, 4H), 4.10 (t, J = 10.2 Hz, 4H), 3.64 (q, J = 7.2 Hz, 4H), 1.32 (t, J = 7.2 Hz, 6H); ^{13}C{^{1}H} (75 MHz, DMSO-d_6): δ 163.4, 54.5, 137.8, 135.6, 131.0, 125.4, 121.6, 114.3, 106.1, 54.9, 48.2, 47.9, 43.6, 12.5: MS(LSIMS) *m*/*z* 591.3641 [$M^{2+} - BPh_4^-$] 591.3659 calcd for [$C_{40}H_{44}BN_4^+$]

5.3. Metallation with $Zr(NMe_2)_4$ and characterization

*5.3.1. Preparation of 2-(1,3-bis(N-butylimidazol-2-ylidene)phenylene)bis(dimethylamido) (iodo)zirconium (IV) (**8**) and 2-(1,3-bis(N-butylimidazol-2-ylidene)-phenylene)(dimethylamido)bis(iodo) zirconium (IV) (**9**)*

1,3-Bis(1-butylimidazol-3-yl) benzene diiodide **7** (100 mg, 0.173 mmol), $Zr(NMe_2)_4$ (115 mg, 0.432 mmol) in CH_2Cl_2 (10 mL) were allowed to react at room temperature for 10 min. The solvent was removed and the residue dried in high vacuum yielding a tan solid (89 mg, 86%). X-ray quality crystals were grown from a saturated methylene chloride solution at room temperature. ^{1}H NMR (CD_2Cl_2) δ 7.66 (d, J = 1.8 Hz, 2H), 7.43 (dd, J = 8.5 Hz, J = 7.27 Hz, 1H), 7.27–7.24 (m, 2H), 4.02 (t, J = 7.4 Hz, 4H), 3.01 (bs, Zr–NCH_3) 1.79 (quintet, J = 7.5Hz, 4H), 1.39 (sextet, J = 7.5 Hz, 4H), 0.99 (t, J = 7.3 Hz, 6H); ^{13}C{^{1}H} (75 MHz, CD_2Cl_2) δ 188.9, 158.2, 148.5, 131.8, 123.4, 116.6, 111.5, 51.7, 38.4, 33.8, 20.3, 13.9.

*5.3.2. Preparation of 2-(1,3-bis(N-butylimidazol-2-ylidene)phenylene) tris(iodo) zirconium (IV) (**10**)*

1,3-Bis(1-butylimidazol-3-yl) benzene diiodide **7** (50 mg, 0.0864 mmol), $Zr(NMe_2)_4$ (58 mg, 0.216 mmol) and CH_2Cl_2 (10 mL) were combined at room temperature for 10 min in the dark. Excess methyl iodide (2.28 g, 16.1 mmol) was added to the pale yellow solution, which produced a cloudy dark yellow suspension, which was stirred for 20 min. The reaction was filtered and then concentrated under vacuum to obtain **10** as a yellow solid (60 mg, 88%). Yellow X-ray quality crystals were grown from a saturated solution of benzene: ^{1}H NMR (C_6D_6) δ 7.05 (t, J = 7.8 Hz, 1H), 6.57 (d, J = 7.8 Hz, 2H), 6.44 (d, J = 1.8 Hz, 2H), 5.92 (d, J = 1.8 Hz, 2H), 4.19 (t, J = 7.6 Hz, 4H), 1.84 (quintet, J = 7.5Hz, 4H), 1.33 (sextet, J = 7.5Hz, 4H), 0.87 (t, J = 7.3 Hz, 6H).; ^{13}C{^{1}H} (75 MHz, CD_2Cl_2) δ 195.5, 164.6, 146.2, 130, 121.3, 115.6, 110.4, 52.2, 33.5, 20.1, 13.7.

*5.3.3. Synthesis of 2-(1,3-bis(N-ethyl-4,5-dihydroimidazol-2-ylidene)phenylene) zirconium (IV) L_n, mixture with (**12**)*

1,3-Bis(*N*-ethylimidazolinium)benzene bis(tetraphenylborate) **11** (61 mg, 0.067 mmol), $Zr(NMe_2)_4$ (91 mg, 0.34 mmol) and C_6D_6 (1 mL) were placed in screw cap vial at room temperature followed by heating for 40 min at 90 °C. The resulting mixture was cooled and the supernatant was removed. The dark brown oil was concentrated. **12**: ^{1}H NMR (CD_2Cl_2) δ 7.46 (s, excess BPh_4^-), 7.15 (t, J = 7.2 Hz, excess BPh_4^-), 6.99 (t, J = 7.2 Hz, excess BPh_4^-), 6.86 (s, mesitylene), 6.36 (d, J = 7.2 Hz, 2H), 6.35 (d, J = 7.2 Hz, 2H), 4.1-2 (multiple peaks), 1.30 (t, J = 7.2 Hz, 6H), 1.24 (t, J = 7.2 Hz, 6H). ^{13}C{^{1}H} NMR (CD_2Cl_2) δ pincer complexes: 214.7, 211.8, 159.8, 158.5, 155.3, 151.1, 150.8, 132.7, 131.7, 131.3, 130.7, 106.6, 105.8, 105.5, 103.3, 96.9, 50.9, 50.4, 45.9, 45.6, 45.1, 44.9, 14.8, 14.6; BPh_4^-: 164.7(q), 136.5, 126.2, 122.3; multiple $Zr(N(CH_3)_2$ peaks: δ 44.5–38.0.

*5.3.4. Synthesis of 2-(1,3-bis(N-ethyl-4,5-dihydroimidazol-2-ylidene)phenylene) tris(dimethylamido) zirconium (IV) (**12**)*

1,3-Bis(*N*-ethylimidazolinium)benzene bis(tetraphenylborate) **11** (62 mg, 0.068 mmol), mesityl lithium (26 mg, 0.204 mmol) and C_6D_6 (1 mL) were placed in screw cap vial at room temperature and were stirred for 10 min. $Zr(NMe_2)_4$ (91 mg, 0.34 mmol) was added and stirring was continued for 30 min at 90 °C. The resulting mixture was cooled and the supernatant was removed. The dark brown oil was concentrated. **12** (80% yield determined by NMR integration): ^{1}H NMR (CD_2Cl_2) δ 7.44 (s, 16H, excess BPh_4^-), 7.25 (t, J = 7.8 Hz, 1H), 7.11 (t, J = 7.2 Hz, excess BPh_4^-), 6.96 (t, J = 7.2 Hz, excess BPh_4^-), 6.86 (s, mesitylene), 6.35 (d, J = 7.8 Hz, 2H), 3.73 (m, 8H), 3.39 (q, J = 7.2 Hz, 4H), 3.30–2.00 (multiple NCH_3 peaks), 1.23 (t, J = 7.2 Hz, 6H); ^{13}C{^{1}H} NMR (CD_2Cl_2) pincer complex ligand: 211.8, 155.3, 151.0, 132.6, 106.6, 50.9, 45.7, 45.6, 14.7; BPh_4^-: δ 164.6(q), 136.5, 126.2, 122.3; mesitylene: 127.3, 21.5; multiple $ZrN(CH_3)_2$ peaks: δ 45.0–38.0.

5.4. Transmetallation to Rh

5.4.1. Synthesis of 2-(1,3-bis(N-butylimidazol-2-ylidene)phenylene)(dimethylammido)bis(iodo) rhodium(III) (**13**) and bis(2-(1,3-bis(N-butylimidazol-2-ylidene)phenylene))bis(μ^2-iodo) dirhodium(III) (**14**)

i. Rh:ligand::1:1. 1,3-bis(1-butylimidazole)benzene diiodide (0.124 g, 0.214 mmol), $Zr(NMe_2)_4$ (0.143 g, 0.535 mmol) and CH_2Cl_2 (10 mL) were stirred for 1 h at room temperature yielding a yellow solution. $[Rh(COD)Cl]_2$ (0.053 g, 0.107 mmol) was added yielding orange solution and stirring was continued for 8 h. The solution was concentrated affording an orange solid. The solid was triturated with pentane (2×10 mL) and after drying yielded an orange solid (0.140 g, 90%). The X-ray quality crystals of **14** were obtained by slow evaporation of a $CDCl_3$ solution.

A portion of the crude orange solid (0.070 g, 0.097 mmol), I_2 (0.058 g, 0.228 mmol) and CH_2Cl_2 (0.7 mL) were shaken vigorously. Excess I_2 was removed by filtration and the volume was reduced. Hexane (5 mL) was added to afford a red crystalline solid (0.060 g, 65%). **13**: ^{1}H NMR (CD_2Cl_2): δ 7.77 (d, $J = 2.1$ Hz, 2H), 7.42–7.47 (m, 3H), 7.31(d, $J = 2.1$ Hz, 2H), 7.23 (d, $J = 2.1$ Hz, 2H), 5.11–5.01 (m, 2H), 4.84 (bs, 1H, H_{N-H}), 4.61–4.51 (m, 2H), 2.09–1.97 (m, 4H), 1.78 (dd, $^3J_{H-H} = 1.5$ Hz, $^3J_{Rh-H} = 4.5$ Hz, 6H), 1.65–1.53 (m, 4H), 1.09 (t, $J = 7.2$ Hz, 6H). $^{13}C\{^1H\}$ NMR ($CDCl_3$): δ 173.7 (d, $J = 39$ Hz, $C_{carbene-Rh}$), 150.8 (d, $J = 40$ Hz, $C_{carbene-Rh}$), 143.6, 124.1, 120.5, 115.1, 108.2, 50.3, 32.3, 18.5, 12.4. MS (LSIMS): **17**: 724 $[M]^+$, 679 $[M - NHMe_2]^+$, 596 $[M - I]^+$, 551 $[M - I - NHMe_2]^+$.

ii. Rh:ligand::2:1. 1,3-bis(1-butylimidazole-3-yl) benzene diiodide (0.124 g, 0.214 mmol), $Zr(NMe_2)_4$ (0.143 g, 0.535 mmol) and CH_2Cl_2 (10 mL) were stirred for 1 h at room temperature yielding a yellow solution. $[Rh(COD)Cl]_2$ (0.106 g, 0.214 mmol) was added, and the solution became intense orange, stirring was continued for 8 h. The solution was concentrated to 5 mL volume and the excess $Zr(NMe_2)_4$ solid was precipitated by stirring the solution with deionized water (0.200 mL) for 15 min. Hexane (10 mL) was added before filtration of the orange solution. The solvent was removed to afford the orange solid (0.122 mg, 66%).

6. X-ray crystallography

The crystals were coated with perfluoropolyethers (PFPE) oil and mounted on to a glass fiber. Measurements were carried out on a Bruker X8 APEX2 (version 1.0-22) [50] KAPPA-CCD X-Ray diffractometer system (Mo-radiation, $\lambda = 0.71073$ Å, 50 KV/30 mA power) for **8**, **9** and **10** and on a Bruker APEX2 (version 1.0-22) [50] platform-CCD X-ray diffractometer system (Mo-radiation, $\lambda = 0.71073$ Å, 50 kV/40 mA power) for compounds **14**. All data were collected at $T = 100(2)$ K. Frames were integrated with the aid of the Bruker SAINT version 7.06A software [51] and using a narrow-frame integration algorithm. The Bruker SHELXTL software package (Version 6.14) [52] was used for phase determination and structure refinement.

For CCC–NHC Zr pincer complexes **8** and **9** a colorless fragment of a prism was used in the analysis. A total of 3373 frames were collected (with a scan width of 0.5° in ϕ using the COSMO strategy in the APEX2 software, and 30 s/frame exposure time). The frames were integrated using the Bruker SAINT software package (version V7.06A) [51] and using a narrow-frame integration algorithm. Based on a monoclinic crystal system, the integrated frames yielded a total of 103964 reflections at a maximum 2θ angle of 72.64° (0.60 Å resolution), of which 12730 were independent reflections ($R_{int} = 0.0254$, $R_{sig} = 0.0144$, redundancy = 8.2, completeness = 100%) and 11390 (89.5%) reflections were greater than $2\sigma(I)$. The unit cell parameters were, $a = 10.3724(5)$ Å, $b = 11.8315(5)$ Å, $c = 21.6021(10)$ Å, $\beta = 98.058(2)°$, $V = 2624.9(2)$ Å^3, $Z = 4$, calculated density $D_c = 1.606$ g/cm^3. Absorption corrections were applied (absorption coefficient $\mu = 1.717$ mm^{-1}; max/min transmission = 0.8443/0.5373) to the raw intensity data using the SADABS program (version 2004/1) [53]. The sample was considered to be a "solid solution" of two different compounds. The major component was 91% of $C_{20}H_{25}N_4ZrI[N(CH_3)_2]_2$ and the minor component was 9% of $[C_{20}H_{25}N_4ZrI_2N(CH_3)_2]$. Note that one of the two $-N(CH_3)_2$ groups of the major component was skewed (and the H-atoms attached to C1# were refined unrestrained, Zr1–C1# distance was 2.690 Å).

For triiodide **10** a colorless fragment of a prism was used in the analysis. A total of 1000 frames were collected (with scan width of 0.5° in ω and ϕ angles of 0°, 90°, 180°, and 270° for every 250 frames, 60 s/frame exposure time). The frames were integrated using the Bruker SAINT software package (version V7.06A) and using a narrow-frame integration algorithm. Based on a monoclinic crystal system, the integrated frames yielded a total of 21289 reflections at a maximum 2θ angle of 52.74° (0.80 Å resolution), of which 6083 were independent reflections ($R_{int} = 0.0264$, $R_{sig} = 0.0278$, redundancy = 3.5, completeness = 99.9%) and 4988 (82%) reflections were greater than $2\sigma(I)$. The unit cell parameters were, $a = 14.863(2)$ Å, $b = 9.0355(14)$ Å, $c = 22.857(4)$ Å, $\beta = 104.273(2)°$, $V = 2974.7(8)$ Å^3, $Z = 4$, calculated density $D_c = 1.946$ g/cm^3. Absorption corrections were applied (absorption coefficient $\mu = 3.504$ mm^{-1}; max/min transmission = 0.8069/0.5196) to the raw intensity data using the SADABS program (version 2004/1) [53].

For CCC–NHC Rh pincer **14** a red fragment of a prism was used for analysis. a total of 2400 frames were

collected for a hemisphere of reflections (with scan width of 0.3° in ω and ϕ angles of 0°, 90°, 180°, and 270° for every 600 frames, 20 s/frame exposure time). The Bruker CELL_NOW program (version 12-31-03) [54] was used to obtain the two different matrices of the rotational twin components (180° rotation about the 1 0 1 real axis). Using the Bruker SAINT software package (version V7.06A) [51] and using a narrow-frame integration algorithm, the frames were first integrated using the first twin domain matrix and then with the second twin domain matrix. Absorption corrections were applied (absorption coefficient $\mu = 3.667$ mm^{-1}; max/min transmission = 0.8210/0.5334) to the raw intensity data using the TWINABS program (version 1.05) [55]. The unit cell parameters were, $a = 12.4710(10)$ Å, $b = 14.8333(12)$ Å, $c = 13.1292(11)$ Å, $\beta = 117.3690(17)°$, $V = 2156.9(3)$ Å^3, $Z = 4$, calculated density $D_c = 2.088$ g/cm^3. A total of 6564 independent reflections at a maximum 2θ angle of 61.00° (0.70 Å resolution) were collected (completeness = 99.8%) and 4853 (73.9%) reflections were greater than $2\sigma(I)$.

Crystallographic data for the structural analyses have been deposited with the Cambridge Crystallographic Data Centre, CCDC No. 262123 for compound **8** and **9**, CCDC No. 262121 for compound **10** and CCDC No. 262122 for compound **14**. These data can be obtained free of charge via www.ccdc.cam.ac.uk or by contacting The Cambridge Crystallographic Data Centre, 12 Union Road, Cambridge CB2 1EZ, UK; fax: +44 1223 336 033.

Acknowledgements

Partial financial support for this work was provided by the National Science Foundation (CHE-0317089), the University of California Energy Institute, the University of California, Cancer Research Coordinating Committee and the Donors of the Petroleum Research fund administered by the American Chemical Society. The authors gratefully acknowledge Mr. Vince Lavallo for a loan of mesityl lithium. The authors gratefully acknowledge Dr. Dan Borchardt for assistance with NMR spectroscopy, and Dr. Rich Kondrat and Mr. Ron New for assistance with mass spectral analyses, and Professor Michael Rettig for a loan of Rh compounds.

References

[1] For recent reviews of carbenes see: D. Bourissou, O. Guerret, F.P. Gabbai, G. Bertrand, Chem. Rev. 100 (2000) 39; G. Bertrand (Ed.), Carbene Chemistry: From Fleeting Intermediates to Powerful Reagents, Marcel Dekker, FontisMedia, 2002.

[2] (a) A. Igau, H. Grutzmacher, A. Baceiredo, G. Bertrand, J. Am. Chem. Soc. 110 (1988) 6463;
(b) A. Igau, A. Baceiredo, G. Trinquier, G. Bertrand, Angew. Chem. 101 (1989) 617;
(c) A.J. Arduengo III, R.L. Harlow, M. Kline, J. Am. Chem. Soc. 113 (1991) 361;
(d) A.J. Arduengo, Acc. Chem. Res. 32 (1999) 913.

[3] For a recent review see: W.A. Herrmann, Angew. Chem. Int. Ed. 41 (2002) 1291.

[4] (a) J.R. Miecznikowski, R.H. Crabtree, Organometallics 23 (2004) 629;
(b) M.T. Powell, D.R. Hou, M.C. Perry, X.H. Cui, K. Burgess, J. Am. Chem. Soc. 123 (2001) 8878;
(c) X.H. Cui, K. Burgess, J. Am. Chem. Soc. 125 (2003) 14212.

[5] (a) O. Navarro, H. Kaur, P. Mahjoor, S.P. Nolan, J. Org. Chem. 69 (2004) 3173;
(b) C. Zhang, J. Huang, M.L. Trudell, S.P. Nolan, J. Org. Chem. 64 (1999) 3804.

[6] (a) S.R. Stauffer, S.W. Lee, J.P. Stambuli, S.I. Hauck, J.F. Hartwig, Org. Lett. 2 (2000) 1423;
(b) J. Huang, G. Grasa, S.P. Nolan, Org. Lett. 1 (1999) 1307.

[7] (a) R.H. Grubbs (Ed.), Handbook of metathesis, Wiley-VCH, Chichester, England, 2003;
(b) L. Jafarpour, S.P. Nolan, J. Organomet. Chem. 617 (2001) 17;
(c) U. Frenzel, T. Weskamp, F.J. Kohl, W.C. Schattenman, O. Nuyken, W.A. Herrmann, J. Organomet. Chem. 586 (1999) 263;
(d) T. Weskamp, F.J. Kohl, W. Hieringer, D. Gleich, W.A. Herrmann, Angew. Chem. Int. Ed. Eng. 38 (1999) 2416.

[8] For a recent example see: P.A. Evans, E.W. Baum, A.N. Fazal, M. Pink, Chem. Commun. (2005) 63.

[9] For a recent report and review see: Y. Canac, M. Soleilhavoup, S. Conejero, G. Bertrand, J. Organomet. Chem. 689 (2004) 3857.

[10] C.J. Moulton, B.L. Shaw, J. Chem. Soc., Dalton Trans. (1976) 1020.

[11] For a review of pincer complexes and their chemistry see: (a) J.T. Singleton, Tetrahedron 59 (2003) 1837;
(b) M.H.P. Rietveld, D.M. Grove, G. vanKoten, New J. Chem. 21 (1997) 751;
(c) C. Kocher, W.A. Herrmann, J. Organomet. Chem. 532 (1997) 261.

[12] For recent examples see: (a) I. Gottker-Schnetmann, P. White, M. Brookhart, J. Am. Chem. Soc. 126 (2004) 1804;
(b) F.C. Liu, A.S. Goldman, Chem. Commun. (1999) 655;
(c) F.C. Liu, E.B. Pak, B. Singh, C.M. Jensen, A.S. Goldman, J. Am. Chem. Soc. 121 (1999) 4086.

[13] (a) M.W. Haenel, S. Oevers, K. Angermund, W.C. Kaska, H.J. Fan, M.B. Hall, Angew. Chem. Int. Ed. 40 (2001) 3596;
(b) C.M. Jensen, Chem. Commun. (1999) 2443.

[14] M.E. O'Neill, K. Wade, The Synthesis, Reactions and Structures of Organometallic Compounds, in: E.W. Abel, F.G.A. Stone, G. Wilkinson (Eds.), Comprehensive organometallic chemistry, vol. 1, Pergamon Press Inc., Elmsford, NY, 1982, pp. 1–43.

[15] For recent pyridyl examples see: (a) D.J. Nielsen, A.M. Magill, B.F. Yates, K.J. Cavell, B.W. Skelton, A.H. White, Chem. Commun. (2002) 2500;
(b) D.S. McGuinness, V.C. Gibson, D.F. Wass, J.W. Steed, J. Am. Chem. Soc. 125 (2003) 12716;
(c) M. Poyatos, J.A. Mata, E. Falomir, R.H. Crabtree, E. Peris, Organometallics 22 (2003) 1110;
(d) M. Poyatos, E. Mas-Marza, J.A. Mata, M. Sanau, E. Peris, Eur. J. Inorg. Chem. (2003) 1215;
(e) D.S. McGuinness, V.C. Gibson, J.W. Steed, Organometallics 23 (2004) 6288.

[16] A.A. Danopoulos, N. Tsoureas, J.A. Wright, M.E. Light, Organometallics 23 (2004) 166.

[17] J.A. Loch, M. Albrecht, E. Peris, J. Mata, J.W. Faller, R.H. Crabtree, Organometallics 21 (2002) 700.

[18] For recently reported xylyl analogues see: (a) S. Grundemann, M. Albrecht, J.A. Loch, J.W. Faller, R.H. Crabtree, Organometallics 20 (2001) 5485;
(b) D.J. Nielsen, K.J. Cavell, B.W. Skelton, A.H. White, Inorg. Chim. Acta 327 (2002) 116;
(c) A.A. Danopoulos, A.A.D. Tulloch, S. Winston, G. Eastham, M.B. Hursthouse, Dalton Trans. 5 (2003) 1009;
(d) A.M. Magill, D.S. McGuinness, K.J. Cavell, G.J.P. Britovsek, V.C. Gibson, A.J.P. White, D.J. Williams, A.H. White, B.W. Skelton, J. Organomet. Chem. 617 (2001) 546.
[19] V.V. Dunina, O.A. Zalevskaya, V.M. Potapov, Russ. Chem. Rev. (Engl. Transl.) 57 (1988) 250.
[20] A.A.D. Tulloch, A.A. Danopoulos, G.J. Tizzard, S.J. Coles, M.B. Hursthouse, R.S. Hay-Motherwell, W.B. Motherwell, Chem. Commun. (2001) 1270.
[21] V.C. Vargas, R.J. Rubio, T.K. Hollis, M.E. Salcido, Org. Lett. 5 (2003) 4847.
[22] L.P. Spencer, S. Winston, M.D. Fryzuk, Organometallics 23 (2004) 3372.
[23] P. Shukla, J.A. Johnson, D. Vidovic, A.H. Cowley, C.D. Abernethy, Chem. Commun. (2004) 360.
[24] For other examples of Group 4 NHC's see: (a) N. Kuhn, T. Kratz, D. Blaser, R. Boese, Inorg. Chim. Acta 238 (1995) 179;
(b) M. Niehues, G. Erker, G. Kehr, P. Schwab, R. Frohlich, O. Blacque, H. Berke, Organometallics 21 (2002) 2905;
(c) M. Niehues, G. Kehr, G. Erker, B. Wibbeling, R. Frohlich, O. Blacque, H. Berke, J. Organomet. Chem. 663 (2002) 192;
(d) A. Weiss, H. Pritzkow, W. Siebert, Eur. J. Inorg. Chem. (2002) 1607.
[25] K. Murata, H. Konishi, M. Ito, T. Ikariya, Organometallics 21 (2002) 253.
[26] P. Wipf, H. Jahn, Tetrahedron 52 (1996) 12853.
[27] For recent examples of zirconium carbene complexes see: Ref. [22] and R.P.K. Babu, R. McDonald, S.A. Decker, M. Klobukowski, R.G. Cavell, Organometallics 18 (1999) 4226.
[28] For a recent report of a CNC–NHC Ti pincer carbene complex see: D.S. McGuinness, V.C. Gibson, J.W. Steed, Organometallics 23 (2004) 6288.
[29] At low temperature a new set of resonances appeared that may be due to the formation of **9**. Detailed study of this observation will be the subject of a future report.
[30] For reports of Group 4 amido ligand exchange see: (a) D.C. Bradley, I.M. Thomas, J. Chem. Soc. (1960) 3857;
(b) J.S.M. Lehn, D.M. Hoffman, Inorg. Chem. 41 (2002) 4063;
(c) S.R. Wade, M.G.H. Wallbridge, G.R. Willey, J. Chem. Soc., Dalton Trans. (1982) 271;
(d) M.D. LoCoco, R.F. Jordan, J. Am. Chem. Soc. 126 (2004) 13918;
(e) M.D. LoCoco, X.W. Zhang, R.F. Jordan, J. Am. Chem. Soc. 126 (2004) 15231;
(f) Z.Z. Wu, J.B. Diminnie, Z.L. Xue, Inorg. Chem. 37 (1998) 2570;
(g) M.H. Chisholm, C.E. Hammond, J.C. Huffman, Polyhedron 7 (1988) 2515;
(h) Y.H. Shi, C.S. Cao, A.L. Odom, Inorg. Chem. 43 (2004) 275, and Ref. [16] therein.
[31] An analysis of Cambridge Crystallographic Database (November 2004) revealed 106 structures with a Zr–Caryl bond. Those that were perfluorinated, were part of a ring of <5 members, were part of a fused ring system of <6 members, or were involved in an ipso interaction (i.e., benzyl substituents) were excluded. The remaining 74 structures had an average Zr–Caryl bond distance of 2.299 Å with a standard deviation of 0.036 Å.
[32] For an example of a long Zr–I bond see: Ref [30b].
[33] (a) L. Pauling, The nature of the chemical bond and the structure of molecules and crystals; an introduction to modern structural chemistry, Cornell University Press, 1960;
(b) T.K. Hollis, J.K. Burdett, B. Bosnich, Organometallics 12 (1993) 3385.
[34] J.M. Tanski, G. Parkin, Organometallics 21 (2002) 587, and Ref. [13] therein.
[35] F. Amor, A. Butt, K.E. duPlooy, T.P. Spaniol, J. Okuda, Organometallics 17 (1998) 5836.
[36] (a) G.J.P. Britovsek, V.C. Gibson, D.F. Wass, Angew. Chem. Int. Ed. 38 (1999) 429;
(b) A.L. McKnight, R.M. Waymouth, Chem. Rev. 98 (1998) 2587.
[37] T.L. Amyes, S.T. Diver, J.P. Richard, F.M. Rivas, K. Toth, J. Am. Chem. Soc. 126 (2004) 4366.
[38] S.M. Lu, H. Alper, J. Am. Chem. Soc. 125 (2003) 13126.
[39] K.W. Aston, S.L. Henke, A.S. Modak, D.P. Riley, K.R. Sample, R.H. Weiss, W.L. Neumann, Tetrahedron Lett. 35 (1994) 3687.
[40] S. Saba, A.M. Brescia, M.K. Kaloustian, Tetrahedron Lett. 32 (1991) 5031.
[41] Details of this investigation will be reported separately.
[42] Y. Yamamoto, K. Maeda, K. Tomimoto, T. Mase, Synlett (2002) 561.
[43] H.M.J. Wang, I.J.B. Lin, Organometallics 17 (1998) 972.
[44] For a recent review and leading references see: P. Wipf, H. Jahn, Tetrahedron 52 (1996) 12853.
[45] (a) S.M. Baxter, G.S. Ferguson, P.T. Wolczanski, J. Am. Chem. Soc. 110 (1988) 4231;
(b) G.S. Ferguson, P.T. Wolczanski, L. Parkanyi, M.C. Zonnevylle, Organometallics 7 (1988) 1967;
(c) P.E. Garrou, in: F.G.A. Stone, R. West (Eds.), Redistribution Reactions of Transition Metal Organometallic Complexes, New York, 1984, pp. 95–129.
[46] See for instance: (a) K.G. Moloy, J.L. Petersen, Organometallics 14 (1995) 2931;
(b) Y.S. Varshavskii, T.G. Cherkasova, Y.T. Struchkov, A.S. Batsanov, L.S. Bresler, N.N. Marasanova, Koord. Khim. (Russ.) (Coord. Chem.) 14 (1988) 1105.
[47] For recent examples see: (a) A.A. Danopoulos, D.M. Hankin, G. Wilkinson, S.M. Cafferkey, T.K.N. Sweet, M.B. Hursthouse, Polyhedron 16 (1997) 3879;
(b) M.K.T. Tin, N. Thirupathi, G.P.A. Yap, D.S. Richeson, J. Chem. Soc. Dalton Trans. (1999) 2947;
(c) M.H. Chisholm, C.E. Hammond, J.C. Huffman, J. Chem. Soc., Chem. Comm. (1987) 1423;
(d) D. Reardon, I. Kovacs, K.B.P. Ruppa, K. Feghali, S. Gambarotta, J. Petersen, Chem. Eur. J. 3 (1997) 1482;
(e) C.E. Laplaza, C.C. Cummins, Science 268 (1995) 861.
[48] Y.J. Ahn, E.B. Bauer, T.K. Hollis, Unpublished results.
[49] A.B. Pangborn, M.A. Giardello, R.H. Grubbs, R.K. Rosen, F.J. Timmers, Organometallics 15 (1996) 1518.
[50] APEX2 Version 1.0-22, Bruker Analytical X-Ray System, Inc., Madison, WI, USA, 2004.
[51] SAINT Software Reference Manual, Version 7.06A, Bruker Analytical X-Ray System, Inc., Madison, WI, USA, 2003.
[52] SHELXTL, Version 6.14, Bruker AXS Inc., Madison, WI, USA, 2003.
[53] SADABS, Version 2004/1, Bruker Analytical X-Ray System, Inc., Madison, WI, USA, 2004.
[54] CELL_NOW, Version 12-31-03, Bruker AXS Inc., Madison, WI, USA, 2003.
[55] TWINABS, Version 1.05, Bruker AXS Inc., Madison, WI, USA, 2004.